Inorg. Chem. **2005**, *44*, 9242–9246

$Ca_6Cu_2Sn_7$: Novel 3D Open Framework with Unusual Sn_4 Tetramers

Zhong-Ming Sun, Sheng-Qing Xia, Yi-Zhi Huang, Li-Ming Wu, and Jiang-Gao Mao*

State Key Laboratory of Structural Chemistry, Fujian Institute of Research on the Structure of Matter, Chinese Academy of Sciences, Fuzhou 350002, P. R. China

Received July 12, 2005

The new ternary polar intermetallic phase, $Ca_6Cu_2Sn_7$, has been synthesized by the solid-state reaction of the stoichiometric mixture of the pure elements in welded Ta tubes at high temperature. Its structure was established by single-crystal X-ray diffraction studies. $Ca_6Cu_2Sn_7$ crystallizes in the monoclinic space group $C2/m$ (No. 12) with cell parameters of $a = 14.257(7)$, $b = 4.564(2)$, and $c = 12.376(7)$ Å, $\beta = 93.979(6)°$, $V = 803.3(7)$ Å^3, and $Z = 2$. The structure of $Ca_6Cu_2Sn_7$ belongs to a new structure type and features a 3D anionic open-framework composed of $[Cu_2Sn_3]$ layers interconnected by unusual Sn_4 tetramers, forming large tunnels along the b axis which are composed of Cu_4Sn_{12} 16-membered rings. The calcium atoms are located in these large tunnels. $Ca_6Cu_2Sn_7$ is metallic and exhibits temperature-independent paramagnetism.

Introduction

Intermetallic phases formed between alkali earth metals (or alkali metals or rare earth metals) and tin are of great research interest because they are rich in structural chemistry and tunable electronic properties.[1] Phase diagram studies indicate that the Ca−Sn system alone exhibits seven intermediate phases.[2,3] Several types of anionic tin oligomers have also been found in these binary and ternary phases.[2,4] Mixing two types of cations with different sizes, such as the combination of alkali earth and alkali metals, two different alkali metals, or two different alkali earth metals, yields a number of polar intermetallics with unusual anionic clusters, chains, and layers.[5−8] The tin-rich binary or ternary phases also are capable of forming type I clathrates featuring cages based on tin pentagons, which possess interesting transport properties.[9]

Pauling's electronegativities of Cu (1.90) and Ni (1.91) are very close to that of Sn (1.96), hence it is expected that a variety of A−Cu(Ni)−Sn (A is alkali earth, alkali or rare earth metal) ternary phases with strong covalent Cu(Ni)−Sn bonding can be formed. Furthermore, the introduction of the transition metals in these systems can also dramatically change the electronic and magnetic properties of the resultant intermetallic compounds.[1] Rare earth copper stannides have been widely investigated because of their interesting magnetic and transport properties.[10] A number of lanthanide−nickel−tin ternary phases, most of them Ni-rich, have also been prepared and their structures elucidated.[11,12] However, alkali earth−Ni(Cu)−Sn ternary phases have been much less

* To whom correspondence should be addressed. E-mail: mjg@ms.fjirsm.ac.cn.

(1) (a) Eisenmann, B.; Cordier, G. In *Chemistry, Structure and Bonding of Zintl Phases and Ions*; Kauzlarich, S. M., Ed.; VCH Publishers: New York, 1996; p 61. (b) Corbett, J. D. In *Chemistry, Structure and Bonding of Zintl Phases and Ions*; Kauzlarich, S. M., Ed.; VCH Publishers: New York, 1996; p 139. (c) Corbett, J. D. *Angew. Chem., Int. Ed.* **2000**, *39*, 670.

(2) (a) Palenzona, A.; Manfrinetti, P.; Fornasini, M. L. *J. Alloys Compd.* **2000**, *312*, 165. (b) Zintl, E.; Neumayr, S. *Z. Elektrochem.* **1933**, *39*, 86. (c) Eckerlin, P.; Meyer, H. J.; Wölfel, E. *Z. Anorg. Allg. Chem.* **1955**, *281*, 322. (d) Ganguli, A. K.; Guloy, A. M.; Leon-Escamilla, E. A.; Corbett, J. D. *Inorg. Chem.* **1993**, *32*, 4349.

(3) (a) Guloy, A. M.; Corbett, J. D. *Z. Anorg. Allg. Chem.* **1992**, *616*, 61. (b) Leon-Escamilla, E. A.; Corbett, J. D. *J. Alloys Compd.* **1998**, *265*, 104. (c) Eckerlin, P.; Leicht, E.; Wölfel, E. *Z. Anorg. Allg. Chem.* **1961**, *307*, 145.

(4) Leon-Escamilla, E. A.; Corbett, J. D. *Inorg. Chem.* **1999**, *38*, 738.

(5) (a) Todorov, I.; Sevov,S. C. *Inorg. Chem.* **2004**, *43*, 6490. (b) Bobev, S.; Sevov, S. C. *J. Alloy Compd.* **2002**, *338*, 87. (c) Bobev, S.; Sevov, S. C. *J. Am. Chem. Soc.* **2002**, *124*, 3359. (d) Bobev, S.; Sevov, S. C. *Inorg. Chem.* **2001**, *40*, 5361.

(6) (a) Bobev, S.; Sevov, S. C. *Inorg. Chem.* **2000**, *39*, 5930. (b) Bobev, S.; Sevov, S. C. *Angew. Chem., Int. Ed.* **2000**, *39*, 4108.

(7) Eisenmann, B.; Schäfer, H. *Z. Anorg. Allg. Chem.* **1974**, *403*, 163.

(8) Ganguli, A. K.; Corbett, J. D.; Köckerling, M. *J. Am. Chem. Soc.* **1998**, *120*, 1223.

(9) (a) Wilkinson, A. P.; Lind, C.; Young, R. A.; Shastri, S. D.; Lee, P. L.; Nolas, G. S. *Chem. Mater.* **2002**, *14*, 1300. (b) Myles, C. W.; Dong, J. J.; Sankey, O. F. *Phys. Rev. B* **2001**, *64*, 165202. (c) Bobev, S.; Sevov, S. C. *J. Solid State Chem.* **2000**, *153*, 92. (d) Nolas, G. S.; Chakoumakos, B. C.; Mahieu, B.; Long, G. J.; Weakley, T. J. R. *Chem. Mater.* **2000**, *12*, 1947. (e) Nolas, G. S.; Weakley, T. J. R.; Cohn, J. L. *Chem. Mater.* **1999**, *11*, 2470.

(10) (a) Fornasini, M. L.; Zanicchi, G.; Mazzone, D.; Riani, P. *Z. Kristallogr. NCS* **2001**, *216*, 21. (b) Fornasini, M. L.; Manfrinetti, P.; Mazzone, D.; Riani, P.; Zanicchi, G. *J. Solid State Chem.* **2004**, *177*, 1919. (c) Szytula, A.; Fus, D.; Penc, B.; Jezierski, A. *J. Alloy Compd.* **2001**, *317−318*, 340. (d) Dörrscheidt, W.; Savelsberg, G.; Stöhr, J.; Schäfer, H. *J. Less-Common Met.* **1982**, *83*, 269.

10.1021/ic051164p CCC: $30.25
Published on Web 10/28/2005

explored.[10b,13,14] It is hoped that the tin-rich phases in the alkali earth−Ni(Cu)−Sn ternary systems will lead to the discovery of novel heteroatomic cluster units, tin oligomers, and intergrowth structures based on novel anionic architectures. Our exploratory studies in the tin-rich alkali earth−Cu−Sn system led to a novel ternary polar intermetallic phase, $Ca_6Cu_2Sn_7$. Its structure features a novel 3D open framework built from ⟨001⟩ $[Cu_2Sn_3]$ layers cross-linked by novel zigzag $[Sn_4]$ tetramers. Herein, we report its synthesis, single-crystal structure, and chemical bonding.

Experimental Section

Preparation of $Ca_6Cu_2Sn_7$. All manipulations were performed inside an argon-filled glovebox with moisture level below 1 ppm. $Ca_6Cu_2Sn_7$ was initially obtained by the solid-state reaction of calcium pieces (0.040 g, 1.0 mmol, 99.98%, Alfa-Aesar), copper powder (0.032 g, 0.5 mmol, 99.999%, Tianjin Fuchen chemical reagent company), and tin granules (0. 178 g, 1.5 mmol, 99.8%, Shanghai fourth chemical reagent company). The sample was loaded into a niobium tube, which was subsequently arc-welded under an argon atmosphere and sealed in an evacuated quartz tube. The mixture was allowed to react at 950 °C for 7 days with prior heating under dynamic vacuum at 300 °C for 1 day. It was then allowed to cool slowly (15 °C/h) to room temperature. Silver gray crystals of $Ca_6Cu_2Sn_7$ were obtained. Several single crystals were analyzed by energy-dispersive X-ray spectroscopy (EDAX 9100), and the results indicate the presence of Ca, Cu, and Sn in a molar ratio of 6.0/2.39/6.6, which is in good agreement with the results of single-crystal structure refinements. After the structural analysis, $Ca_6Cu_2Sn_7$ was prepared in high yield and high purity by reacting a stoichiometric mixture of the pure metals at 950 °C for 3 days and annealing them at 700 °C for 10 days (purity ca. 90% with a small amount of copper and Nb_3Sn as well as other unidentified impurities, Nb came from the Nb tube). To eliminate the Nb_3Sn impurity, $Ca_6Cu_2Sn_7$ was subsequently prepared using Ta tubes under same conditions as that for using the Nb tubes. XRD powder diffraction study indicates that the product is much more pure than that prepared using Nb tubes. The experimental XRD powder pattern matches well with the one simulated from the X-ray single-crystal structural analysis (see Supporting Information), but a very small amount of copper still exists. The purity of the sample is estimated to be about 95% on the basis of the ratio of the intensity of the strongest peak from the impurities to that of the strongest reflection for $Ca_6Cu_2Sn_7$.

(11) (a) Zhuravleva, M. A.; Bilc, D.; Mahanti, S. D.; Kanatzidis, M. G. *Z. Anorg. Allg. Chem.* **2003**, *629*, 327. (b) Skolozdra, R. V.; Mandzyk, V. M.; Aksel'rud, L. G. *Kristallogr.* **1981**, *26*, 480. (c) Rossi, R.; Marazza, R.; Ferro, R. *J. Less-Common Met.* **1985**, *107*, 99. (d) Dwight, A. E. *Proc. Rare Earth Res. Conf., 11th* **1974**, *2*, 642. (e) Chevalier, B.; Etourneau, J. *J. Mater. Chem.* **1999**, *9*, 1789.

(12) (a) Gil, A.; Penc, B.; Baran, S.; Hernandez-Velasco, J.; Szytula, A.; Zygmunt, A. *J. Alloys Compd.* **2003**, *361*, 32. (b) Sichevich, O. M.; Komarovskaya, L. P.; Grin', Y. N.; Yarmolyuk, Y. P.; Skolozdra, R. V. *Ukr. Fiz. Zh. (Ukr. Ed.)* **1984**, *29*, 1342. (c) Skolozdra, R. V.; Komarovskaya, L. P. *Ukr. Fiz. Zh. (Ukr. Ed.)*, **1983**, *28*, 1093. (d) Komarovskaya, L. P.; Aksel'rud, L. G.; Skolozdra, R. V. *Z. Kristallogr.* **1983**, *28*, 1201. (e) Chevalier, B.; Fourgeot, F.; Laffargue, D.; Gravereau, P.; Fournés, L.; Etourneau, J. *J. Alloy Compd.* **1997**, *262−263*, 114. (f) Skolozdra, R. V.; Mandzyk, V. M.; Gorelenko, Y. K.; Tkachuk, V. D. *Fiz. Met. Metalloved.* **1981**, *52*, 966.

(13) (a) Dörrscheidt, W.; Schäfer, H. *J. Less-Common Met.* **1978**, *58*, 209. (b) Rahlfs, P. *Metallwirtsch. Metallwiss. Metalltech.* **1937**, *16*, 640. (c) Boudard, M.; Doisneau, B.; Audebert, F. *J. Alloys Compd.* **2004**, *370*, 169.

(14) (a) May, N.; Schäfer, H. *Z. Naturforsch.* **1974**, *B29*, 20. (b) Osamura, K.; Murakami, Y. *J. Less-Common Met.* **1978**, *60*, 311.

Table 1. Summary of Cell Parameters, Data Collection, and Structure Refinements for $Ca_6Cu_2Sn_7$

empirical formula	$Ca_6Cu_2Sn_7$
fw	1198.39
space group	*C*2/*m* (No. 12)
a (Å)	14.257(7)
b (Å)	4.564(2)
c (Å)	12.376(7)
β (deg)	93.979(6)
V (Å^3)	803.3(7)
Z	2
D_{calcd} (g cm^{-3})	4.954
temp (K)	293(2)
μ (mm^{-1})	15.155
GOF on F^2	1.027
R1, wR2 ($I > 2\sigma(I)$)[a]	0.0254/0.0606
R1, wR2 (all data)	0.0308/0.0624

[a] $R1 = \sum||F_o| - |F_c||/\sum|F_o|$, $wR2 = \{\sum w[(F_o)^2 - (F_c)^2]^2/\sum w[(F_o)^2]^2\}^{1/2}$.

Table 2. Atomic Coordinates and Equivalent Thermal Parameters ($\times 10^3$ Å^2) for $Ca_6Cu_2Sn_7$

atom	site symmetry	*x*	*y*	*z*	*U*(eq)[a]
Ca(1)	4i	0.1373(1)	1/2	0.0031(1)	11(1)
Ca(2)	4i	0.4621(1)	0	0.2994(1)	11(1)
Ca(3)	4i	0.1948(1)	0	0.2931(1)	12(1)
Cu(1)	4i	0.3305(1)	1/2	0.3888(1)	13(1)
Sn(1)	4i	0.3180(1)	1/2	0.1756(1)	9(1)
Sn(2)	4i	0.5104(1)	1/2	0.1181(1)	9(1)
Sn(3)	4i	0.1595(1)	1/2	0.4816(1)	10(1)
Sn(4)	2d	1/2	1/2	1/2	14(1)

[a] *U*(eq) is defined as one-third of the trace of the orthogonalized U_{ij} tensor.

Crystal Structure Determination. A silver gray single crystal of $Ca_6Cu_2Sn_7$ with dimensions of 0.20 × 0.16 × 0.10 mm^3 was selected from the reaction product and sealed into a thin-walled glass capillary under an argon atmosphere. Data collection was performed on a Rigaku Mercury CCD (Mo Kα radiation, graphite monochromator) at 293(2) K. The data set was corrected for the Lorentz factor, polarization, air absorption, and absorption caused by variations in the path length through the detector faceplate. An absorption correction based on the multiscan method was also applied.[15a]

The space group for $Ca_6Cu_2Sn_7$ was determined to be *C*2/*m* (No. 12) on the basis of systematic absences, *E* value statistics, and the satisfactory refinements for the structure. The structure was solved using direct methods (SHELXTL) and refined by least-squares methods with atomic coordinates and anisotropic thermal parameters.[15b] All atomic sites are fully occupied according to the site occupancy refinements. Final difference Fourier maps showed featureless residual peaks of 2.112 and −1.614 e Å^{-3} (0.91 and 0.80 Å, respectively away from Sn(4) and Sn(3)). Some of the data collection and refinement parameters are summarized in Table 1. Atomic coordinates and important bond lengths and angles are listed in Tables 2 and 3, respectively. More details of the crystallographic studies and atomic displacement parameters are given in the Supporting Information.

Magnetic Property Measurements. Magnetic susceptibility measurements on polycrystalline samples of $Ca_6Cu_2Sn_7$ were performed with a PPMS-9T magnetometer at a field of 5000 Oe in the temperature range of 2−300 K.

Extended Hückel Band Calculations. Three-dimensional band structure calculations for $Ca_6Cu_2Sn_7$ along with the density of states

(15) (a) *CrystalClear*, version 1.3.5; Rigaku Corp.: Woodlands, TX, 1999. (b) Sheldrick, G. M. *SHELXTL, Crystallographic Software Package*, version 5.1; Bruker-AXS; Madison, WI, 1998.

Table 3. Selected Bond Lengths (Å) and Angles (deg) for $Ca_6Cu_2Sn_7$.

Ca(1)−Sn(1)	3.229(2)	Ca(1)−Sn(1)	3.271(2) (×2)
Ca(1)−Sn(2)	3.296(2) (×2)	Ca(1)−Sn(2)	3.384(2) (×2)
Ca(2)−Cu(1)	3.200(2) (×2)	Ca(2)−Sn(2)	3.306(2) (×2)
Ca(2)−Sn(3)	3.318(2)	Ca(2)−Sn(1)	3.368(2) (×2)
Ca(2)−Sn(4)	3.388(2) (×2)	Ca(2)−Sn(3)	3.482(2)
Ca(3)−Cu(1)	3.168(2) (×2)	Ca(3)−Sn(1)	3.281(2) (×2)
Ca(3)−Sn(2)	3.289(2)	Ca(3)−Sn(3)	3.326(2) (×2)
Ca(3)−Sn(3)	3.359(2)	Cu(1)−Sn(1)	2.633(2)
Cu(1)−Sn(4)	2.696(1)	Cu(1)−Sn(3)	2.766(2)
Cu(1)−Sn(3)	2.787(1) (×2)	Sn(1)−Sn(2)	2.881(2)
Sn(2)−Sn(2)	2.917(2)	Sn(3)−Sn(4)	3.241(1) (×2)
Sn(3)···Sn(3)	3.451(1) (×2)		
Sn(1)−Cu(1)−Sn(4)	120.50(4)	Sn(1)−Cu(1)−Sn(3)	114.56(4)
Sn(4)−Cu(1)−Sn(3)	124.94(5)	Sn(1)−Cu(1)−Sn(3)	125.04(3) (×2)
Sn(4)−Cu(1)−Sn(3)	72.44(2) (×2)	Sn(3)−Cu(1)−Sn(3)	76.84(3) (×2)
Sn(3)−Cu(1)−Sn(3)	109.91(5)	Cu(1)−Sn(1)−Sn(2)	104.36(3)
Sn(1)−Sn(2)−Sn(2)	102.43(3)	Cu(1)−Sn(3)−Cu(1)	103.16(3) (×2)
Cu(1)−Sn(3)−Cu(1)	109.91(5)	Cu(1)−Sn(3)−Sn(4)	132.25(2) (×2)
Cu(1)−Sn(3)−Sn(4)	122.95(3) (×2)	Cu(1)−Sn(3)−Sn(4)	52.48(3) (×2)
Sn(4)−Sn(3)−Sn(4)	89.51(4)	Cu(1)−Sn(4)−Cu(1)	180.00(3)
Cu(1)−Sn(4)−Sn(3)	124.92(3) (×4)	Cu(1)−Sn(4)−Sn(3)	55.08(3) (×4)
Sn(3)−Sn(4)−Sn(3)	89.51(4) (×2)	Sn(3)−Sn(4)−Sn(3)	180.0 (×2)
Sn(3)−Sn(4)−Sn(3)	90.49(4) (×2)		

Table 4. Atomic Parameters Used for Extended Hückel Calculations on $Ca_6Cu_2Sn_7$[a]

atom type	orbital	H_{ii} (eV)	ξ_1	ξ_2	c_1	c_2
Ca	s	−7.0000	1.2000		1.000	
	p	−4.0000	1.2000		1.000	
Cu	s	−11.400	2.2000		1.000	
	p	−6.0600	2.2000		1.000	
	d	−14.000	5.9500	2.300	0.5933[b]	0.5744[b]
Sn	s	−16.160	2.1200		1.000	
	p	−8.3200	1.8200		1.000	

[a] H_{ii} values are the diagonal matrix elements $\langle\chi_i|H^{\text{eff}}|\chi_i\rangle$, where H^{eff} is the effective Hamiltonian. In our calculations of the off-diagonal matrix elements $H_{ij} = \langle\chi_i|H^{\text{eff}}|\chi_j\rangle$, the weighted formula was used. [b] Contraction coefficients of the d orbits used in the double-ξ Slater-type orbital.

(DOS) and crystal orbital overlap population (COOP) curves were performed by using the Crystal and Electronic Structure Analyzer (CAESAR) package.[16] The atomic parameters used in the calculations along with the H_{ii} and Slater exponents are presented in Table 4. Double-ξ expansions were used for the d orbitals of the copper atom.

Results and Discussion

$Ca_6Cu_2Sn_7$ belongs to a new structure type. Its structure features a 3D novel open framework built by ⟨001⟩ [Cu_2Sn_3] layers interconnected by novel zigzag [Sn_4] tetramers (Figure 1a).

The ⟨001⟩ [Cu_2Sn_3] layer can also be viewed as the copper atoms being placed above and below the tin square sheet (Figure 1b). Within the ⟨001⟩ [Cu_2Sn_3] layer, the interconnection of Cu(1) and Sn(3) atoms leads to a 1D [Cu_2Sn_2] "ladder" along the *b* axis; these ladders are further cross-linked by Sn(4) atoms via Cu−Sn and Sn−Sn bonds into a 2D architecture (Figure 1b). This type of connectivity also results in slightly distorted 2D square sheets of tin that are normal to the *c* axis. Cu(1) is 1.429 Å off the plane formed by 3 Sn(3) and 1 Sn(4) atoms. The Sn−Sn distance (Sn(3)−Sn(4)) within the vacant [Sn_4] square is 3.241(1) Å, and the

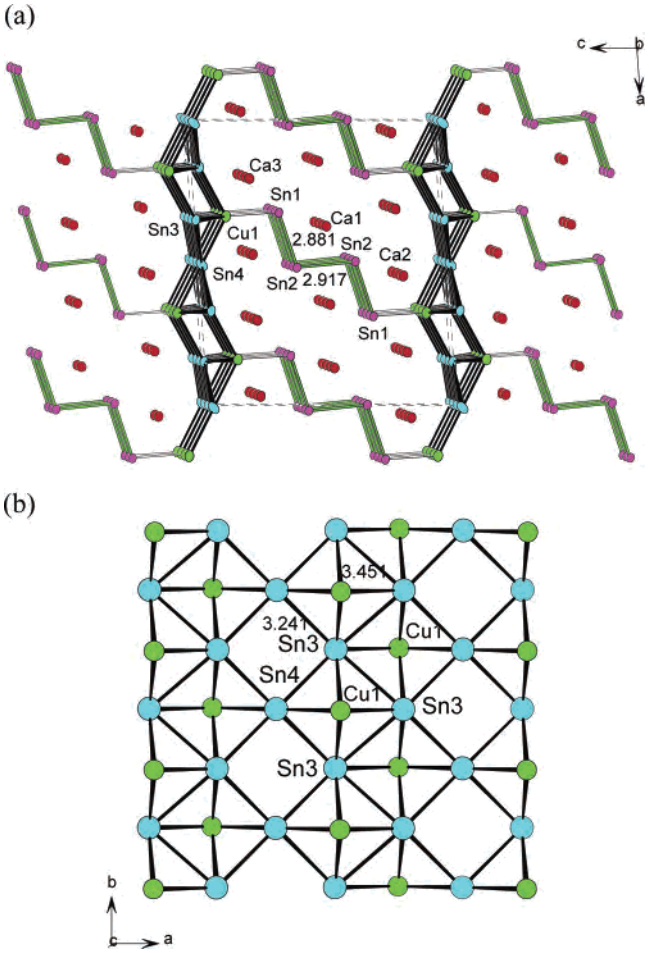

Figure 1. View of the structure of $Ca_6Cu_2Sn_7$ along the *b* axis (a) and a Cu_2Sn_3 layer (b). The thermal ellipsoids are drawn at 75% probability.

one (Sn(3)−Sn(3)) for the [Sn_4] square containing a copper atom above or below is 3.451 (1) Å. The former is slightly longer than that for the square sheet in $ThSn_2$ (3.126 Å),[17] whereas the latter is very close to that for the tin square sheets in $BaMg_2Sn_2$.[7] The Cu−Sn distances are in the range of 2.696(1)−2.787(1) Å. These Cu−Sn bond lengths are comparable to those reported in other Cu−Sn phases.[10,14] A similar [Cu_2Sn_3] layer can be found in $Yb_4Cu_2Sn_5$; however, each pair of copper atoms from two neighboring [Cu_2Sn_2] ladders are further bridged by a [Sn_2] dimer (Sn−Sn 2.877 Å).[10a] The [Cu_2Sn_3] layer in $Ca_6Cu_2Sn_7$ can be also considered to be formed by removing one-third of the copper atoms from the [CuSn] 2D layer in $AeCuSn_2$ (Ae = Ba, Sr), whose structure features 2D [CuSn] layers cross-linked by 1D zigzag [Sn] chains that are parallel to the 2D layer,[14a] resulting in shorter Sn−Sn contacts within the vacant Sn_4 square (Figure 2).

The zigzag [Sn_4] tetramer is composed of 2 Sn(1) and 2 Sn(2) atoms (Figure 1a), which can be considered to be a fragment cut from 1D zigzag {Sn^{2-}} chain in AeSn (Ae = Ca, Sr, Ba).[2,18] To our knowledge, such a zigzag tin tetramer has not been reported before. The Sn−Sn distances within

(16) Ren, J.; Liang, W.; Whangbo, M.-H. *CAESAR for Windows*; Prime-Color Software, Inc., North Carolina State University: Raleigh, NC, 1998.

(17) Cirafici, S.; Palenzona, A.; Manfrinetti, P. *J. Less-Common Met.* **1983**, *90*, 49.

(18) Merlo, F.; Fornasini, M. L. *J. Less-Common Met.* **1967**, *13*, 603.

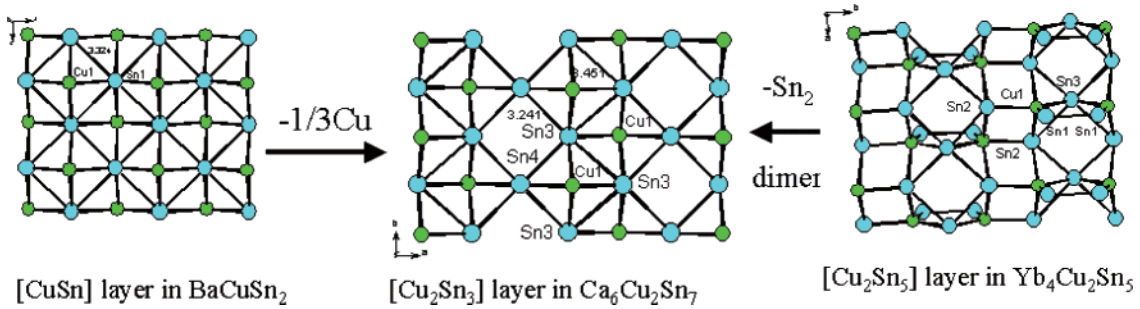

Figure 2. $[Cu_2Sn_3]$ layer in $Ca_6Cu_2Sn_7$ and its relationship to the [CuSn] layer in $BaCuSn_2$ and the $[Cu_2Sn_5]$ layer in $Yb_4Cu_2Sn_5$.

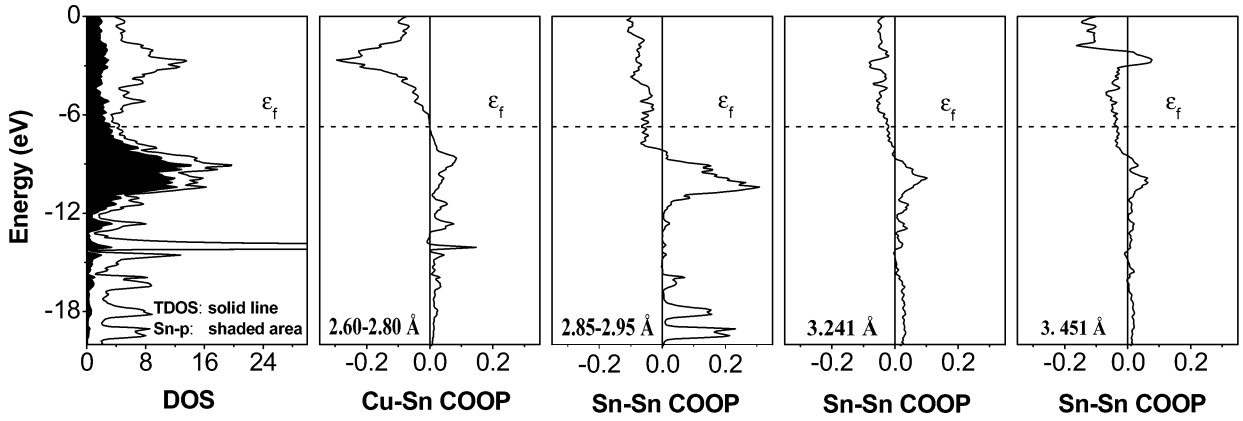

Figure 3. Density of states (DOS) and crystal orbital overlap population (COOP) curves for $Ca_6Cu_2Sn_7$. The Fermi level is set at −6.71 eV.

the zigzag $[Sn_4]$ tetramer are 2.881(2) and 2.917(2) Å, respectively, which are significantly shorter than those for the ⟨001⟩ $[Cu_2Sn_3]$ layer, but they are comparable to those in BaSn (2.917 Å).[18] These Sn−Sn distances within the Sn_4 tetramer are also slightly longer than the Sn−Sn single bond distance of 2.81 Å observed in the diamond modification of α-Sn.[19] The Sn−Sn−Sn angle of 102.43(3)° within the $[Sn_4]$ tetramer is significantly smaller than that in BaSn (105.93°).[18] It should also be mentioned that both the Sn_5 pentamer in $Ca_{31}Sn_{20}$ and the Sn_6 hexamer in $A_{36}Sn_{23}$ (A = Yb, Ca) are linear with Sn−Sn−Sn bond angles of 180°.[2a,4]

The above two types of building blocks in $Ca_6Cu_2Sn_7$ are further interconnected via Cu−Sn bonds (2.633(2) Å) into a novel three-dimensional open framework with long narrow tunnels along the *b* axis (Figure 1a). The long narrow tunnel is composed of $[Cu_4Sn_{12}]$ 16-membered rings. The size of the tunnel is estimated to be 5.0 × 13.5 Å^2 on the basis of structural data. All calcium atoms are located at the above tunnels (Figure 1a). Ca(1) is surrounded by 7 Sn atoms (3 Sn(1) + 4 Sn(2)), whereas Ca(2) atom is in close contact with two copper and eight tin atoms. Ca(3) is 8 coordinated by two copper and six tin atoms. The Ca−Sn and Ca−Cu distances are in the ranges of 3.229(2)−3.388(2) Å and 3.168(2)−3.200(2) Å, respectively. The copper atom is in a distorted $[Sn_5]$ square pyramidal geometry, and it is also in contact with four Ca atoms (2Ca(2) + 2Ca(3)). The Sn−Cu−Sn bond angles range from 72.44(2) to 125.04(3)°. The four crystallographically independent Sn atoms have different coordination geometries. Sn(1) is in contact with 1 Cu, 1 Sn, and 7 Ca atoms, whereas Sn(2) is 9 coordinated by 2 Sn and 7 Ca atoms. Sn(3) is surrounded by 4 Sn, 3 Cu, and 5 Ca atoms, whereas Sn(4) has 2 Cu, 4 Sn, and 4 Ca atoms as its neighbors.

To understand the chemical bonding in $Ca_6Cu_2Sn_7$, three-dimensional band structure calculations were performed by using the semiempirical extended Hückel methods. $Ca_6Cu_2Sn_7$ is metallic with no band gaps around the Fermi level (Figure 3). The states just below and above the Fermi level are mainly from the p orbitals of the Sn atoms mixing with a small amount of the s and p orbitals of the transition metals, as well as a small amount of the s and p orbitals from the calcium atoms.

Semiempirical COOP allows for a more quantitative bond analysis (Figure 3). The Sn−Sn bonds (2.881−2.918 Å) within the $[Sn_4]$ tetramer have a large average overlap population (OP) value of 0.658. The average OP values for the Sn−Sn bonds within the $[Cu_2Sn_3]$ layer are 0.29 and 0.12 for Sn(3)−Sn(4) (3.241 (1) Å) and Sn(3)−Sn(3) (3.451(1) Å), respectively, indicating that these bonds are much weaker than those within the Sn_4 tetramer. The Cu−Sn bonds (2.632−2.787 Å) with an average OP value of 0.34 are significantly bonding. The Ca−Sn bonds (3.177−3.412 Å) are weakly bonding with a small overlap population value of 0.167, and the Ca−Cu bonds with a very small OP value of 0.027 are essentially nonbonding. The calculated Mulliken charges are +1.09, +1.23, and +1.10 for Ca(1), Ca(2) and Ca(3), respectively, indicating that the electron transfer from calcium atoms to the 3D anionic open framework is incomplete, probably because of the significant Ca−Sn bonding. The calculated Mulliken charge for the copper atom is −1.25, and the "apparent" negative charge is probably

(19) Donohue, J. *The Structures of the Elements*; Wiley: New York, 1974.

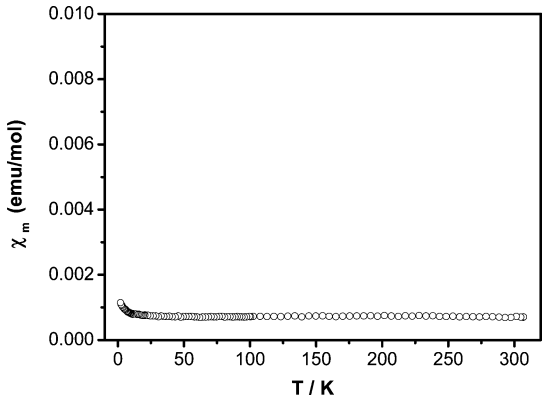

Figure 4. Molar susceptibility of $Ca_6Cu_2Sn_7$ as a function of temperature.

related to the significant Cu−Sn bonding. The calculated Mulliken charges are −1.03, −0.78, −0.24, and −0.26 for Sn(1), Sn(2), Sn(3), and Sn(4), respectively. The more negative charges for the tin atoms within the Sn_4 tetramer are the result of the fewer copper and tin neighbors around them.

$Ca_6Cu_2Sn_7$ exhibits temperature-independent paramagnetism in the temperature range of 10−298 K (Figure 4), which is typical for a metallic compound. Its molar susceptibility at 300 K is 7.0×10^{-4} emu mol^{-1}, which is typical for a polar intermetallic compound that exhibits temperature-independent paramagnetism. The slight increase of the molar susceptibility below 10 K is the contribution of a small amount of copper impurity. These results are in good agreement with the results from the band structure calculations.

In summary, we have successfully obtained a novel tin-rich ternary phase, $Ca_6Cu_2Sn_7$, with a new structure type. Its structure features a novel 3D open framework built by $\langle 001 \rangle$ $[Cu_2Sn_3]$ layers interconnected by unusual zigzag $[Sn_4]$ tetramers. $Ca_6Cu_2Sn_7$ is metallic and displays the temperature-independent paramagnetism.

Acknowledgment. This work is supported by National Natural Science Foundation of China (Grant Nos. 20371047 and 20573113) and NSF of Fujian Province (No. E0420003).

Supporting Information Available: Figures showing the coordination geometries around Ca, Sn and Cu atoms, lists of atomic displacement parameters, simulated and experimental XRD powder patterns, as well as X-ray crystallographic files for $Ca_6Cu_2Sn_7$ in CIF format. This material is available free of charge via the Internet at http://pubs.acs.org.

IC051164P